CHALMERS | UNIVERSITY OF GOTHENBURG

PREPRINT 2010:7

Wiener Chaos Expansions for Estimating Rain-flow Fatigue Damage in Randomly Vibrating Structures with Uncertain Parameters

SUNETRA SARKAR
SAYAN GUPTA
IGOR RYCHLIK

Department of Mathematical Sciences
Division of Mathematical Statistics
CHALMERS UNIVERSITY OF TECHNOLOGY
UNIVERSITY OF GOTHENBURG
Gothenburg Sweden 2010

Preprint 2010:7

Wiener Chaos Expansions for Estimating Rain-flow Fatigue Damage in Randomly Vibrating Structures with Uncertain Parameters

Sunetra Sarkar, Sayan Gupta, Igor Rychlik

Department of Mathematical Sciences
Division of Mathematical Statistics
Chalmers University of Technology and University of Gothenburg
SE-412 96 Gothenburg, Sweden
Gothenburg, February 2010

Preprint 2010:7
ISSN 1652-9715

Matematiska vetenskaper
Göteborg 2010

Wiener Chaos Expansions for Estimating Rain-flow Fatigue Damage in Randomly Vibrating Structures with Uncertain Parameters

Sunetra Sarkar [a,*] Sayan Gupta [b] Igor Rychlik [c]

[a] *Department of Aerospace Engineering, Indian Institute of Technology Madras, Chennai 600036 India*

[b] *Department of Applied Mechanics, Indian Institute of Technology Madras, Chennai 600036 India*

[c] *Mathematical Sciences, Chalmers University of Technology, SE-412 96, Gothenbourg, Sweden*

Abstract

The problem of estimating the fatigue damage in randomly vibrating structures with uncertain parameters is considered. The loadings are assumed to be stationary and Gaussian. The corresponding accumulated fatigue damage is described through the rain-flow cycle counting algorithm. For stationary and ergodic loads, the accumulated rain-flow fatigue damage can be estimated if the system and the load spectrum are known. However, these estimates would be erroneous if the structure properties and/or the spectrum parameters of the loading are significantly uncertain. Corrections to account for the parameter uncertainties is usually obtained using the Gauss error propagation formula, and is accurate for small parameter variations. An alternative approach based on Wiener Chaos expansions is employed to estimate the rain-flow fatigue damage in linear/nonlinear structural systems with parameter uncertainties. The performance of the proposed approach is compared with the Gauss error propagation formula. The proposed method is illustrated through fatigue damage estimation of three simplified examples involving a moving vehicle on a rough road, Morison's force due to random sea waves and the blade of a wind turbine.

Key words: Random fatigue, Gaussian loads, Wiener Chaos, rain-flow damage, wind turbines, fluid-structure interaction, Morison's force, vehicular vibrations, damage rate

1 Introduction

Fatigue is the process of initiation and growth of cracks in a material, usually metal, due to variable fluctuating stresses. Fatigue damage gradually accumulates over time leading to changes in the material locally. When the damage exceeds certain threshold levels, the crack growth process becomes unstable leading to accelerated growth causing sudden structural failures. Since the onset of unstable crack growth can be triggered even for small loadings, it becomes very important in any safety analysis to estimate the fatigue damage in existing structures and make accurate predictions about the expected fatigue lifetime.

Estimates of the expected fatigue lifetime of any component in an existing structure are based on models to describe the fatigue process. The models used are often empirical, such as, the Wöhler curves in conjunction with Palmgren-Miner's linear damage accumulation rule [1, 2], or the Paris-Erdogan crack growth equation [3]. These methods give predictors of fatigue life and the simplest approach to assess the safety is to compare how much the expected fatigue life is greater than the design life. The design safety margin depends on the conservatism in the expected fatigue life in comparison to the design life and depends on the design target safety level and the different sources of uncertainties affecting the value of the predictor. The uncertainties that need to be quantified are: variability in the material micro-structure, variability in manufacturing of the material, quality of production of components (variability in geometry), initial crack length, modeling errors of fatigue phenomenon, errors in modeling stresses at "hot spots" and uncertainty in prediction of future loads.

For estimating the rain-flow fatigue damage, the variability of the stress is described by means of rainflow matrices, or rainflow range distributions which measure the extent of stress fluctuations at a randomly chosen time during the design life. The distribution is then used to compute the average rate of fatigue damage growth d. It is often assumed that, under stationary conditions, the fatigue damage accumulation can be assumed to be deterministic if the parameters of the system and the loading are known, predicting the expected fatigue life is still an exercise in uncertainty quantification as the future load parameters (spectrum) are unknown. However the computation of the rainflow range distribution is a complicated task. For stationary Gaussian loads and linear structures, the rate of damage growth is constant and several approximations have been proposed to compute the expected rate of damage

* Corresponding author: sunetra.sarkar@gmail.com, Phone: +91 44 2257 4024, FAX: +91 44 2257 4002

Email addresses: sunetra.sarkar@gmail.com (Sunetra Sarkar), gupta.sayan@gmail.com (Sayan Gupta), rychlik@chalmers.se (Igor Rychlik).

growth if the power spectral function is known. Here, we shall use the simple bound proposed in [4] called today the narrow band approximation; see [5]. Though the method is mostly used for Gaussian processes, the bound is valid for any process having symmetrical and unimodal upcrossing intensity.

Other source of uncertainties include errors in structure models. Here, structures will be described by means of suitable systems of linear or non-linear differential equations. The parameters in the equations (mass, stiffness and damping) may not be exactly known and hence the stress properties (like damage growth rate) becomes uncertain. The primary focus of this paper is on studying the effect of uncertainties of the system parameters on the expected fatigue damage. Assuming certain simplifying conditions, the fatigue damage is expressed in terms of the damage growth rate. The fatigue damage growth rate is expressed as a complicated function of the uncertain system parameters, modeled as random variables. In this paper, we adopt the so called Wiener chaos expansions [6–9] to express the expected fatigue damage rate in terms of the uncertain random variables.

1.1 The Wiener Chaos expansion

The Wiener Chaos method, also popularly known as the method of polynomial chaos expansions, is a promising tool for solving a wide variety of problems involving stochastic partial differential equations. This method was originally developed by Wiener [6] and involves spectral representation of the uncertainty in terms of orthogonal polynomials of random variables. In its original form, the expansion employs Hermite polynomials as basis from the Askey scheme and Gaussian random variables. Subsequently, Cameron and Martin [8] developed a more explicit formulation for the Wiener-Hermite expansion based on an explicit discretization of the white noise process through its Fourier expansion.

The Wiener chaos approach has been used for solving elliptic partial differential equations with random coefficients [9]. The random coefficients are first expanded in terms of independent Gaussian random variables using Karhunen-Loeve expansions. The random solution was presented as a Hermite expansion of these random variables. This was also known as the stochastic finite element method. Since then, spectral polynomial chaos based approaches for non-Gaussian processes with other random basis functions have also been used in various problems of practical interest.

In this study, we use the methodology for studying the dependence of the fatigue damage in a vibrating system to a parameter modeled as uncertain. We consider the simpler random variable model where the relationship between

the damage and the uncertain parameter is expressed as function of a random variable. Thus, a random function $X(Z)$ with $\mathsf{E}[X(Z)^2] < \infty$, where Z is a standard normal random variable, can be written in terms of Wiener-Chaos expansions as

$$X(Z) = \sum_{j=0}^{\infty} c_j H_j(Z), \tag{1}$$

where, H_j are Hermite polynomials and $c_j = \mathsf{E}[X(Z)H_j(Z)]$. The first few normalized Hermite polynomials are given by

$$\begin{aligned} &H_0(z) = 1, \quad H_1(z) = z, \quad H_2(z) = (z^2 - 1)/\sqrt{2}, \\ &H_3(z) = (z^3 - 3z)/\sqrt{6}, \quad H_4(z) = (z^4 - 6z^2 + 3)\sqrt{24}, \quad \ldots \end{aligned} \tag{2}$$

Higher order Hermite polynomials can be generated from the following recursive relationship,

$$\sqrt{n+1}H_{n+1}(z) = zH_n(z) - \sqrt{n}H_{n-1}(x). \tag{3}$$

It must be noted that the condition $\mathsf{E}[X(Z)^2] < \infty$ implies that the truncated polynomials in Eq. (1) converges in L^2 to $X(Z)$. The rate of convergence is quite fast if the function $X(Z)$ is smooth. The condition $\mathsf{E}[X(Z)^2] < \infty$, however, does not require the function $X(Z)$ to be continuous. The exponential convergence of the polynomial chaos expansion has been extended to several other types of commonly used probability distributions. One can use orthogonal polynomials from the generalized Askey scheme for some standard non-Gaussian input uncertainty distributions, such as, gamma and beta random variables [10].

1.2 Fatigue damage rate

Though many methods have been discussed in the literature for approximating the damage rate for Gaussian loads, the number of methods applicable for non-Gaussian loads are much less. A review of these methods is outside the scope of this paper. However, we mention the method proposed in [11], where the Hermite polynomials have been used to obtain the distribution of the damage. Here, the author first approximated the probability distribution function (PDF) of the response using Hermite expansions. Subsequently, the expansion has been used to find the distribution of the load cycles and finally, the distribution of the damage rate. This is a different application of the Hermite expansion than used in this paper. Here, the Hermite polynomial expansion is not used to approximate the damage rate d, but to describe the dependence of the damage rate $d(\boldsymbol{\Theta})$ on some uncertain parameters represented through the vector $\boldsymbol{\Theta}$. We assume that $\boldsymbol{\Theta}$ is a function of independent

standard normal variables $\mathbf{Z} = (Z_1, \ldots, Z_n)$. Since $\mathbf{\Theta} = \mathbf{\Theta}(\mathbf{Z})$, we have that damage rate d is a function of $\mathbf{Z}$. (The derived relation can be used for any deterministic value of parameters $\mathbf{\Theta} = \theta$, however the mean square error is minimal if $\mathbf{Z}$ is Gaussian). In the following, for simplicity of exposition only, we assume that $\mathbf{Z}$ is one dimensional and represent the vector as the random variable Z.

A commonly used methodology to describe the function $d(Z)$ is to employ the Gauss error propagation formula, viz.

$$d(z) \approx d(0) + \frac{\partial d}{\partial z}(0)\, z + \frac{1}{2}\frac{\partial^2 d}{\partial z^2}(0)\, z^2 = d_G(z). \tag{4}$$

In the above equation, often the quadratic term is neglected due to uncertainties in estimation of the second order derivative. If $\mathsf{E}[d(Z)^2] < \infty$, then an alternative approach could be followed using the Hermite polynomial expansion

$$d(z) = \sum_{j=0}^{\infty} c_j H_j(z) \approx \sum_{j=0}^{n} c_j H_j(z) = d_n(z). \tag{5}$$

Here, H_j are normalized Hermite polynomials, and hence, $c_j = \mathsf{E}[d(Z)H_j(Z)]$. It is desirable that the function $d(z)$ should be sufficiently smooth for fast convergence of the Hermite expansion of $d(z)$; this is however, not a necessary requirement. For one dimensional Z,

$$c_j = \frac{1}{\sqrt{2\pi}} \int_{-\infty}^{+\infty} d(z) H_j(z) e^{-z^2/2}\, \mathrm{d}z \approx \frac{1}{\sqrt{2\pi}} \sum_{i=1}^{n} h_i d(z_i) H_j(z_i) e^{-z_i^2/2}, \tag{6}$$

where, (h_i, z_i) is some quadrature scheme. Here, we replaced the infinite integration region by the interval $[-4, 4]$ and employed Gauss quadrature with $n = 20$. Note that it is important to control whether

$$\sum_{i=1}^{n} h_i H_j(z_i)^2 \frac{1}{\sqrt{2\pi}} e^{-z_i^2/2} \approx 1. \tag{7}$$

Comparing the two approximations in Eq. (4) and Eq. (5), one can say that the first one requires less evaluations of the function $d(z)$, but is more sensitive to errors in computed (estimated) values of the d-function. This can be an important issue if the damage rate has to be evaluated using ergodicity assumption from observed or simulated stress functions. Next, locally the function can have "wrong" curvature and hence high order Taylor formulas would be required to get sufficient accuracy in Eq. (4). Obviously high order derivatives are more difficult to estimate numerically.

In this paper the two approaches will be compared for three illustrative problems. The first example considers the fatigue damage in a vehicle traveling in a rough road. Here, the vehicle is modeled as a linear system excited by Gaussian forcing. In the second example, we consider the fatigue damage due to

sea wave loadings. The wave loads are modeled as Morrison's force. Here, the force is calculated as a nonlinear transformation of wave velocities modeled as Gaussian processes, and are therefore, non-Gaussian. Finally, we consider the fatigue damage in a blade of a wind turbine. The problem is modeled as a fluid structure interaction problem and is highly nonlinear. As a result, the Gauss error propagation formula is not a suitable approximation.

The paper is organized as follows: In the following, basic fatigue is reviewed together with the general definition of the rainflow cycle count method and some properties of rainflow cycles, and safety index methodology. Next, we illustrate the use of the proposed method for responses of linear structural systems excited by Gaussian loads. In the next section, we extend the application areas to include a problem involving linear behavior but non-Gaussian loads and a problem involving a highly nonlinear problem subjected to Gaussian excitation. The salient observations arising from this study is summarized in the concluding section. Three appendices are presented at the end.

2 Review of Fatigue

Fatigue testing of components has traditionally been carried out using constant amplitude stress cycles. In these experiments the stress is oscillating between a minimum and a maximum value until fatigue failure occurs. Usually sinusoidal cycles are considered in these tests; however, the shape of the cycles in most cases have been observed to have insignificant influence. Repeating the experiments for different amplitudes, but keeping the ratio between the minimum and the maximum load, denoted as R, constant, results in what is known as Wöhler curves. These curves are also referred to as the S-N curves, show a log-linear dependence between the number of cycles to failure, N, and the stress cycle range, s, and is expressed as

$$\log(N) = a - k\log(s) + \varepsilon, \tag{8}$$

where, the parameters $a > 0$ and $k \geq 1$ depend on the material properties and the stress ratio R. Material properties which have little or no influence in the static case, such as the smoothness of the metal surface, residual tensions and size and geometry of the structure, may greatly influence the fatigue life. The total error due to scatter in material properties, modelling errors etc. is represented by the term $\varepsilon \in N(0, \sigma_\varepsilon^2)$.

However, in real life applications, loads usually do not exhibit constant amplitude sinusoids but are instead random processes, such as, ocean waves and wind loads acting on the offshore located wind power turbines or vehicle loads due to a random road surface. Here, we assume that the material stress is

proportional to the displacements with a constant c which depends on the structure properties. Often, approximate methods, such as the Finite Element Method, are needed for the computation of the constant c. Here, the structure response, usually the displacements, are described by a set of differential equations, where the external loads are the inputs. If the differential equations are linear, the responses are referred to as *linear responses* while if the differential equations are nonlinear the responses will be termed as *nonlinear responses*.

For random processes, the load cycles and cycle ranges need to be defined using an appropriate cycle counting procedure. Just as in the case of constant amplitude loadings, even for random loadings, the local maxima and minima are of importance in characterizing the fatigue damage and the shape of the cycles have relatively less influence on the fatigue life. Though several cycle counting algorithms have been discussed in the literature, the rainflow cycle counting method has been shown to be the most accurate. The method was originally introduced by Endo: The first paper in English can be found in [12]. Here, we shall use the alternative definition given in [13], which is more suitable for statistical analysis, see Appendix I.

Fatigue damage from variable amplitude (random) loads is commonly regarded as a cumulative process. Using the linear Palmgren-Miner damage accumulation rule together with Eq. (8), the total damage $D^{\text{tot}}(t)$ at time t, can be defined as

$$D^{\text{tot}}(t) = \sum e^{-a} \, (c \, h_i)^k. \tag{9}$$

The parameters $a > 0$ and $k \geq 1$ are the same parameters as in Eq. (8) and have traditionally been estimated using constant amplitude test for some value of the stress ratio R. Since the ratio R for the cycles of a random process varies, the estimation of parameters a and k is difficult. Different correction factors have been proposed in the literature. Fatigue failure is normally predicted when $D^{\text{tot}}(T)$ equals one, although in practice, fatigue failure may occur for $D^{\text{tot}}(T)$ between, say, 0.3 and 3. Hence, a direct application of Eq. (9) may give less accurate predictions. Other factors to consider are as listed in [14]. A possible solution to incorporate these factors in the model is to estimate the parameters a, k of the S-N curve using tests with variable amplitude loads similar to the real load processes. However, discussions on this issue is beyond the scope of this paper.

2.1 Probability for fatigue failure

In some situations one wishes to more accurately measure the risk for failure and would like to check whether the probability for failure of a component before time T, say one year, is below 10^{-3} or some other small value. To measure small risks one needs to consider different sources of uncertainties,

e.g., uncertainties in geometry, material, statistical errors in estimation of the S-N curve as well as modeling errors.

When computing failure probabilities or safety indices, it is more convenient to use the so called *nominal damage* $D(T) = e^a\, c^{-k} D^{\text{tot}}(T)$. Further, the stress proportional constant, c, is an uncertain parameter as a result of variability in geometry, manufacturing variability between components and model error. Hence the risk of fatigue failure thus depends on the following parameters or random variables: a, k (material strength), c (stress proportionality - geometrical uncertainties), $D(T)$ accumulated nominal damage, e material variability (residuals between S-N data and fitted S-N curve).

A simple measure of reliability against fatigue failure is the so-called Cornell's safety index, which measures the 'distance' from the mean location to failure, expressed in number of standard deviations and is defined by [16]

$$I_C = \frac{\mathsf{E}[A] - \ln(\mathsf{E}[D(T)])}{\sqrt{\sigma_A^2 + R[D(T)]^2}}. \tag{10}$$

Here, A is a function of the material parameters and $R[D(T)]$ is the coefficient of variation of $D(T)$. Alternative definitions of the safety index have been proposed in the literature, see [17] for a review. However, for the sake of simplicity, in this paper we limit our focus to the Cornell's safety index only. We also assume that k is known ($k = 3$ in all the examples). Knowing the index risk for fatigue failure can be approximated by $P_f \approx \Phi(-I_C)$, where $\Phi(\cdot)$ is the standard normal PDF.

For stationary loadings, the nominal damage $D(t)$ grows linearly with the damage rate d, *i.e.*, the expected damage in time interval of length t is equal to $d \cdot t$. Further, for ergodic loads (or when the coefficient of variation of the damage decreases to zero as t tends to infinity), one may assume that the damage $D(t) \approx d\, t$, if the length of stationarity period t is long enough. Hence often $R[D(T)]$ is much smaller than σ_A and can be neglected. However, apart from the uncertainties in the loading, there could be other sources of uncertainties, such as, uncertainties in the system parameters which significantly affect the fatigue damage and $R[D(T)]$ may no longer be negligible which should be calculated for safety assessments.

2.1.1 Locally stationary loads

If the environmental loads changes slowly and the mean stresses are approximately constant, then one can for simplicity, split the service time T, into N stationary periods of lengths Δt_i. Assuming that Δt_i are sufficiently long, the total nominal damage $D(T) \approx \sum d_i \Delta t_i$. Here, d_i are the damage rates which depend on the properties of the external loads and, sometimes, on the degree

of the deterioration of the structure. Even if the structural deterioration is neglected, still the damages d_i are deterministic but maybe unknown, because of uncertainties in the future loads.

A standard approach to resolve this problem is to parameterize loads. However, if the environment varies in a stationary way (for example, missions and owners do not change), then one can use the so called long-term distributions of the parameters to compute the expected damage

$$\mathsf{E}[D(T)] = T\,\mathsf{E}_{\text{long-term}}[d_i]. \tag{11}$$

The damage rates d_i still have to be estimated for the different external loading conditions. The most reliable way to estimate d is to measure stresses. However, this is not always possible, *e.g.*, at the design stage, and hence the computations of d is based on mathematical models of stress variabilities. Hence, there is apparent risk for modeling errors.

Consequently, beside the parameters describing uncertain environment, one may consider additionally, parameters in the governing differential equations describing the system, as uncertain too. We shall not differentiate between the two type of parameters and gather them in a vector $\boldsymbol{\Theta}$. As mentioned in the introduction we shall consider a simplified situation of one dimensional Θ and that Θ is a function of a normal variable $m + \sigma\, Z$, where Z is standard Gaussian. Consequently the uncertainty in the value of the damage rate during a stationarity period is modelled by $d(m+\sigma\, Z)$. Note that the values of m, σ, Z may change for different stationarity periods, i.e.

$$D(T) = \sum d(m_i + \sigma_i\, Z_i)\Delta t_i = \sum d_i(Z_i)\Delta t_i, \tag{12}$$

say. Now, using Eq. (5) to express the damage rate d_i for the i-th stationary segment, one can express as

$$d_i(Z_i) = \sum_{j=0}^{\infty} c_{ij} H_j(Z_i). \tag{13}$$

It is obvious that Eq. (13) can be used in a truncated form.

Computations of $R[D(T)]^2$ can be quite complex and depend on a particular application. For example if the mass of the system is uncertain because of variability in manufacturing then $d_i = d_i(Z)$ and

$$D(T) = \sum_{i=1}^{\infty}\sum_{j=1}^{\infty} \Delta t_i c_{ij} H_j(Z) = \sum_{j=1}^{\infty} H_j(Z) \left(\sum_{i=1}^{\infty} \Delta t_i c_{ij}\right) = \sum_{j=1}^{\infty} c_j\, H_j(Z),$$

say. Hence, with $c_0 = \sum_{i=1}^{\infty} \Delta t_i c_{i0}$

$$R[D(T)]^2 = \sum_{j=1}^{N} (c_j/c_0)^2, \tag{14}$$

which is likely to be large. Here, the damage rate d_i for all the intervals are functions of the same variable Z. On the other hand, if we use a parameter to model the mass variability because of fluctuations say, in the cargo weight, the parameter can be modeled by random variables Z_i corresponding to each interval. It can be reasonably assumed that the Z_i are independent, leading to

$$R[D(T)]^2 = \frac{\sum_{i=1}^{N} \Delta t_i^2 \sigma^2(i)}{\left(\sum_{i=1}^{N} \Delta t_i m(i)\right)^2}, \tag{15}$$

where $\sigma^2(i) = \sum_{j=1}^{\infty} c_{ij}^2$, and $m(i) = c_{i0}$. In the latter case, the coefficient of variation $R[D(T)]^2$ is likely to be negligible for large N.

In this paper we just illustrate possibilities of computing the covariance $R[D(T)]$. The focus of the rest of this paper is devoted to computing the variability of the damage rates d. We assume that the loading conditions are stationary and that the external loadings are suitably modeled as Gaussian random processes. We will use Wiener chaos based expansions to quantify the variability of the damage rates d, first, for linear responses and subsequently, for nonlinear responses.

3 Linear responses

As is well known, for linear structures with stationary Gaussian loads, the responses (stresses) are also stationary and Gaussian. In such cases, the damage rate d can be bounded using the narrow band approximation proposed in [4]. More precisely, let $\mu(u)$ be the expected number of times a stationary process passes level u, in the upward direction, in an unit interval. For zero mean stationary stress with symmetrical crossing intensity $\mu(u)$, *i.e.*, $\mu(u) = \mu(-u)$ Bendat [4] proposed to approximate the damage rate as

$$d \approx \int_0^{\infty} 2k(2u)^{k-1} \mu(u)\, \mathrm{d}u. \tag{16}$$

In [5], it was demonstrated that actually the narrow band approximation in Eq. (16) is a bound, and can be mathematically written as

$$d \leq \int_0^{\infty} 2k(2u)^{k-1} \mu(u)\, \mathrm{d}u = d^{\mathrm{nb}}. \tag{17}$$

For a stationary and Gaussian stress $Y(t)$, with spectral power density $S_\sigma(\omega)$, the upcrossing intensity is given by the Rice formula [18], and as shown in [5],

can be written as

$$\int_0^\infty 2k(2u)^{k-1}\mu(u)\,\mathrm{d}u = \frac{2^{(3/2)k}\Gamma(1+k/2)}{2\pi}\sqrt{\lambda_2}\,\lambda_0^{(k-1)/2} = d^{\mathrm{nb}}, \qquad (18)$$

where

$$\lambda_n = \int_0^{+\infty} \omega^n S_\sigma(\omega)\,\mathrm{d}\omega. \qquad (19)$$

Obviously, the uncertainty in d is related to the variability of the first two spectral moments in the stress spectrum.

It must be noted that Bendat's approximation given by Eq. (16) is still applicable for slightly nonlinear responses of Gaussian excitations; see Example 2. However, when the response is a highly nonlinear function of the Gaussian forcing (Example 3), one may need to use Monte Carlo simulations in conjunction with empirical estimates of the damage rate d. These issues will be discussed later in the paper.

3.1 Example 1: Road and vehicle stress spectra

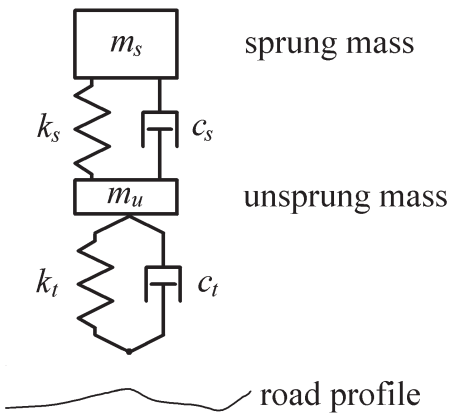

Symbol	**Value**	**Unit**
m_s	3400	kg
k_s	270 000	N/m
c_s	6000	Ns/m
m_u	350	kg
k_t	950000	N/m
c_t	300	Ns/m

Fig. 1. Example 1: A schematic diagram of the quarter vehicle model and the parameter values.

We first consider the problem of estimating the fatigue damage in a vehicle traveling in a rough road condition. The fatigue damage is assessed by modeling the vehicle as a quarter-vehicle traveling at constant velocity on rough road profiles. This very simple model cannot be expected to predict loads on a physical vehicle exactly, but will highlight the most important characteristics as far as fatigue damage accumulation is concerned.

The quarter vehicle model is modeled to consist of two masses, one "unsprung" mass m_u, representing the mass of the wheel etc. and one sprung mass m_s,

representing the vehicle mass; see Fig. 1. The stiffness and the damping of the vehicle is represented by the spring of stiffness k_s and the damper c_s. The tire stiffness and damping are respectively modeled through the spring of stiffness k_t and damper c_t. The transfer function for the quarter vehicle model can be written as

$$H(\omega) = \frac{m_s\omega^2(k_t + i\omega c_t)}{k_t - \frac{(k_s+i\omega c_s)\omega^2 m_s}{m_s\omega^2 - k_s - i\omega c_s} - m_u\omega^2 + i\omega c_t}\left(1 + \frac{m_s\omega^2}{k_s - m_s\omega^2 + i\omega c_s}\right). \quad (20)$$

We use the parameter values shown in Fig. 1. These parameters are set to mimic heavy vehicle dynamics and have been proposed in [19].

To model the road roughness, we use the commonly used Gaussian road surface model presented in [20], and given by the following equation

$$S^{\text{MIRA}}(\xi) = \begin{cases} 10^{a_0}(\frac{\xi}{\xi_0})^{-w_1} & , \xi \in [0.01, 0.2], \\ 10^{a_0}(\frac{\xi}{\xi_0})^{-w_2} & , \xi \in [0.2, 10], \\ 0 & , \text{otherwise}, \end{cases} \quad (21)$$

with typical values of $a_0 = -5$, $w_1 = 3$, $w_2 = 2$ and reference spatial frequency $\xi_0 = 0.2\ \text{m}^{-1}$. The load spectrum for a vehicle at speed θ, can thus be expressed as

$$S^{\text{vehicle}}(\omega) = \frac{1}{\theta}|H(\omega)|^2 S^{\text{MIRA}}\left(\omega/(2\pi\theta)\right), \quad (22)$$

where, $\xi = \omega/(2\pi\theta)$.

In order to assess vehicle fatigue damage, the total force, $Y(t)$, for $t \in [0, T]$, acting on the sprung mass is rainflow-counted. The damage rate d is approximated using the narrow band approximation d^{nb}, discussed in Eqs. (18-19). We are interested in the influence of the velocity θ on the damage rate. We assume that the car velocity Θ to be a random variable, such that, it can be represented as $\Theta = m + \sigma Z$, where Z is a standard Gaussian variable, $m = 25$ and $\sigma = 5$. This implies that the velocity varies between $[55, 125]$ km/hr with high probability ($\pm 2\sigma$). Using Eqs. (5-6), the damage rate approximation by the Hermite model is given by

$$d_3^{\text{nb}}(Z) = 0.0793 + 0.0395\ H_1(Z) + 0.0098\ H_2(Z) + 0.0010\ H_3(Z). \quad (23)$$

Here, the suffix 3 in d_3^{nb} indicates a three term Hermite polynomial expansion. The corresponding two term approximation using the Gauss formula is

$$d_G^{\text{nb}}(Z) = 0.0753 + 0.0396 \cdot Z + 0.0143 \cdot Z^2/2. \quad (24)$$

As can be seen in Fig. 2, the estimates d_3^{nb} and d_G^{nb} are practically equivalent.

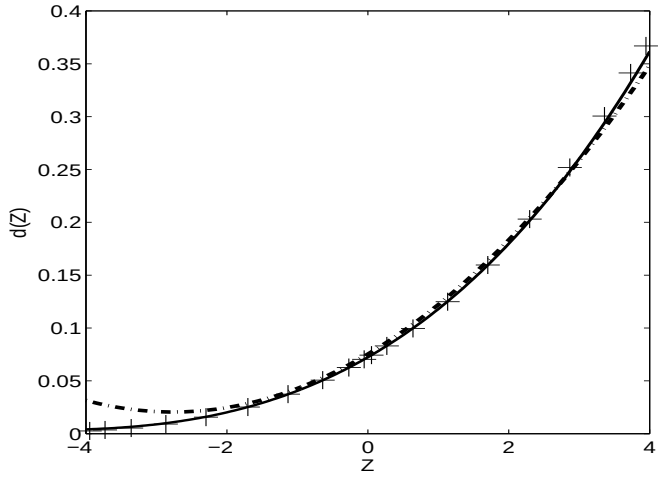

Fig. 2. Example 1: Fatigue damage in a vehicle; crosses: The nominal narrowband damage rate $d^{\mathrm{nb}}(Z)$ for the linear model of car suspension as a function of the random variable, Z; solid line: Hermite polynomial expansion of the damage rate $d_3^{\mathrm{nb}}(Z)$; dashed dotted: the Gauss error propagation approximation d_G^{nb}.

4 Nonlinear responses

In this section, we consider two different classes of nonlinear responses. The first problem belongs to the class of transformed Gaussian processes where the response is a memoryless function of the vector valued Gaussian processes. The second type is when the function has a memory and typically involves structural systems whose governing equations of motion are nonlinear.

4.1 Example 2: Non-Gaussian Morison's force

The wave force acting on a tubular section of an offshore structure is often described by the so called Morison's equation. Let $X(t)$ be the velocity of sea fluid around a circular pile representing a supporting pile of an offshore structure, and $F(t)$ be the force acting on the pile. By Morison's equation, the force, $F(t)$, is equal to the following function of the process $X(t)$,

$$F(t) = K_M X'(t) + K_D X(t)|X(t)|, \tag{25}$$

where K_M, K_D are positive constants. Usually, $X(t)$ is modeled as a random process having the Pierson-Moskowitz spectrum (see Appendix II). In ocean engineering literature, it is often assumed that $X(t)$ is a stationary Gaussian process. For simplicity only, we consider normalized velocity, *i.e.*, we assume that $\mathsf{E}[X(t)] = 0$ and $\mathsf{V}[X(t)] = \mathsf{V}[X'(t)] = 1$, and that the nominal damage is computed for the force

$$F(t) = X'(t) + K\, X(t)|X(t)|. \tag{26}$$

The upcrossing intensity for the structure response can be expressed in terms of the following integral

$$\mu(u) = \beta \int_{-\infty}^{+\infty} e^{-\frac{1}{2}(y^2+(u-Ky|y|)^2)} \Psi\left(\frac{\alpha}{\sqrt{1-\alpha^2}}(y - 2K|y|u + 2K^2y^3)\right) \mathrm{d}y, \tag{27}$$

where, $\Psi(y) = \phi(y) + y\Phi(y)$, where $\phi(\cdot)$ and $\Phi(\cdot)$ respectively being the standardized normal probability density function (pdf) and PDF. Here, $\beta = \frac{1}{2\pi}\sqrt{\lambda_4 - 1}$, while α is the irregularity factor $\alpha = 1/\sqrt{\lambda_4}$. Finally, the damage intensity can be bounded by means of narrow band bound in Eq. (17), viz. $d \leq d^{\mathrm{nb}} = \int_0^\infty 2k(2u)^{k-1}\mu(u)\,\mathrm{d}u$, (here $k = 3$).

Suppose $K = m + \sigma\, Z$, where Z is standard normal variable. We wish to quantify how this uncertainty influences the damage rate d^{nb}. Before we investigate this problem, we first check whether d^{nb} is a useful bound. In Fig. 3, 100 rainflow damage rates, represented by dots, for random parameter K estimated from 2.5 hour long Morison's force have been shown. The variations in the estimated damage rates are obviously due to statistical errors because of the finite simulation length. The corresponding narrow band bounds d^{nb} are represented as crosses. One can see that the conservatism of the bound is moderate and that due to statistical errors, estimates of the rainflow damage rate can occasionally be larger then the bounds. Since the bound is a smoother function of K than the estimates of the rainflow damage rates, the bound will be used to get the Hermite polynomial expansion (Wiener chaos).

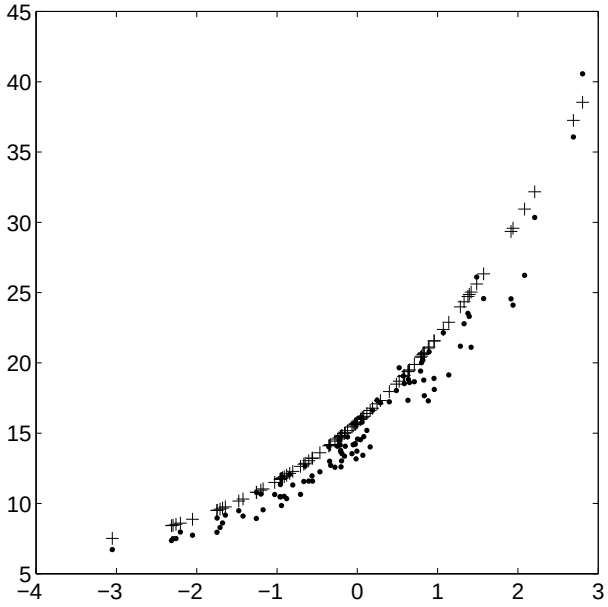

Fig. 3. Example 2: Fatigue damage due to Morison's force; Dots: Hundred nominal rainflow damage rates estimated from 2.5 hour long simulated Morison's forces with random parameter K; Crosses: the corresponding narrow band bound of the damages.

The truncated Hermite polynomials expansion of the $d^{\mathrm{nb}}(Z)$ is given by Eq. (5), where, $c_j = \mathsf{E}[d^{\mathrm{nb}}(Z)H_j(Z)]$. The coefficients are evaluated from the following integrals

$$c_j = \frac{\beta}{\sqrt{2\pi}} \int_{-\infty}^{+\infty} \int_{0}^{\infty} \int_{-\infty}^{+\infty} 2k(2u)^{k-1} H_j(y) e^{-\frac{1}{2}(z^2+(u-(m+\sigma\, y)z|z|)^2)} \times \Psi\left(\frac{\alpha}{\sqrt{1-\alpha^2}}(z - 2(m+\sigma\, y)|z|u + 2(m+\sigma\, y)^2 z^3)\right) \phi(y)\, \mathrm{d}z\, \mathrm{d}u\, \mathrm{d}y. \tag{28}$$

which need to be computed numerically. Here, since the kernel is Gaussian, the outer integral is evaluated using the Gauss quadrature scheme.

For $K = m + \sigma\, Z$, where Z is standard normal variable, with $m = 0.5$ and $\sigma = 0.1$, the three term truncated Hermite expansion is given by

$$d_3^{\mathrm{nb}}(Z) = 16.727 + 5.235\, H_1(Z) + 1.308\, H_2(Z) + 0.082\, H_3(Z). \tag{29}$$

In Fig. 4, the values of d^{nb} at quadrature nodes are marked by crosses, while the truncated Hermite expansion $d_3^{\mathrm{nb}}(Z)$ is shown by the solid line. As in the previous example, the agreement between these two estimates is good. The simpler two term Gauss error propagation formula, gives the following model

$$d_G^{\mathrm{nb}}(Z) = 15.781 + 5.088\, Z + 0.955\, Z^2. \tag{30}$$

The $d_G^{\mathrm{nb}}(Z)$ is shown as dashed doted line in Fig. 4. We observe that the Gauss error approximation becomes less accurate as the variation of Z increases from the mean value. While it is obvious that the Hermite poynomial based expansion is more accurate, the Gauss approximation is sufficiently useful provided that the variation of Z around the mean value is small.

4.2 Example 3: Fatigue damage in a wind turbine blade

In this example, we investigate the fatigue damage in a wind turbine blade. For simplicity of the analysis of the wind turbine blade, we consider a strip of unit span along the blade having a symmetric airfoil profile. This implies that the problem is simplified to the 2-D case. We use a turbine blade flutter model in which the blade section oscillates in pitch. This is a classical stall flutter case in which an airfoil (blade profile) oscillates in the rotational direction in a highly separated flow-field in which the viscous effects are strong. One would typically need to solve the Navier-Stokes equation or use an experiment based semi-empirical model to calculate the aerodynamic loads time histories.

In the present study, we consider a 1000 KW wind turbine with rotors of 50 m diameter having a semispan of 0.8 m at 0.75 radial distance (design section)

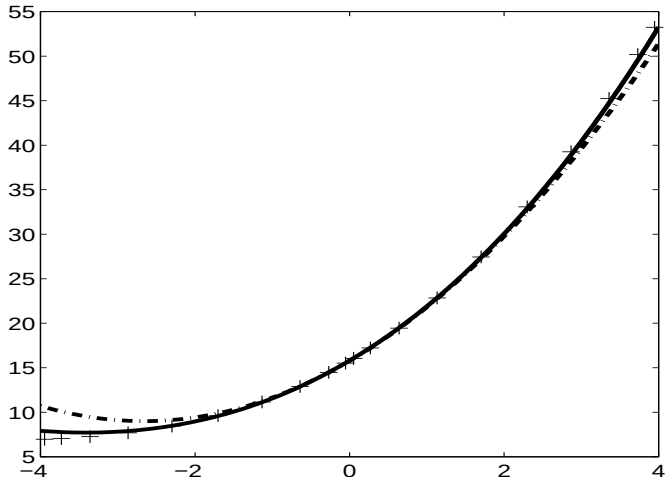

Fig. 4. Example 2: Fatigue damage due to Morison's force; crosses: The nominal narrowband damage rate $d^{\mathrm{nb}}(Z)$ as a function of the random variable Z; solid line: the $d_3^{\mathrm{nb}}(Z)$ Hermite polynomial expansion of the damage rate; dashed dotted: the Gauss error propagation approximation d_G^{nb}.

and rotational natural frequency of about 3.9 rad/sec. The rated speed is 25.4 RPM and the upper limiting operating speed is about 25 m/s while the survival speed of the rotor is designed to be 70 m/s (assumed to occur very rarely). A typical section of the turbine blade represents a symmetrical airfoil. We consider a NACA 0012 profile for the airfoil. A schematic plot of the airfoil and its coordinate system is shown in Fig. 5. The relative wind velocity $\bar{V}$ is the resultant of the local wind velocity V_g and the blade rotational velocity Ω.

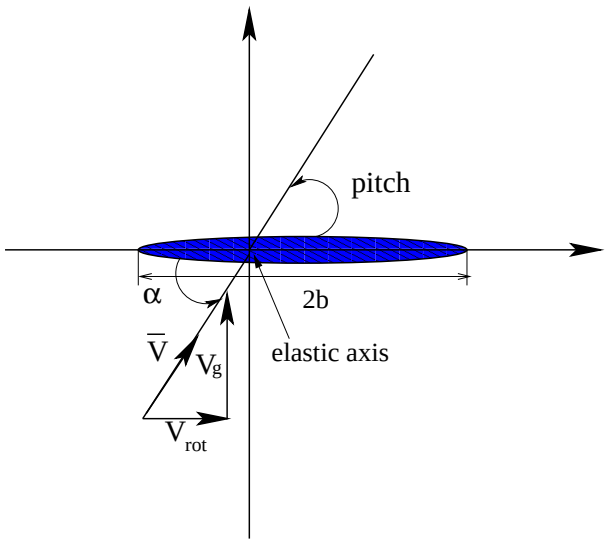

Fig. 5. A schematic diagram of the flutter model with a NACA 0012 profile.

The airfoil oscillates in the rotational degree-of-freedom about its elastic axis point and has rotational stiffness. Except for this, the airfoil is otherwise as-

sumed to be rigid. The equation of motion for the single degree-of-freedom pitching oscillation is given by [24, 25]:

$$I_\alpha \ddot{\alpha} + I_\alpha \omega_\alpha^2 \alpha = M(t) + F\sin(\omega t). \tag{31}$$

Here, α is the effective angle of attack defined as the angle that the resultant wind velocity $\bar{V}$ makes with the blade longitudinal axis, I_α is the sectional mass moment of inertia, ω_α is the natural frequency of the pitch elastic mode, $M(t)$ is the time dependent aerodynamic moment, and $F\sin(\omega t)$ is an externally applied moment. (Sometimes a concentrated structural nonlinearity is also included to model the large twisting of the blades [21]. This is often a standard way to model the effect of various control mechanisms that may be present on the blades [22, 23]. However, in the present model we consider the effects of aerodynamic nonlinearity only.)

A non dimensional form of the governing equation in Eq. (31) is often helpful in aeroelastic analysis to investigate the effect of system parameters. Thus, we introduce non dimensional time $\tau = t\bar{V}/b$, where, b is the airfoil semi-chord and $\bar{V}$ is the resultant head wind acting at a specific section (element) and is defined by

$$\bar{V} = \sqrt{V_{\rm rot}^2 + V_g^2}. \tag{32}$$

Here, V_g is the average speed of the head gusts, $V_{\rm rot}$ is the rotational velocity and is given by $V_{\rm rot} = \Omega \times r$, where, r is the radial length of the blade section from the hub, and Ω is the angular velocity of the blade rotations.

Following [24, 25], the non dimensionalized form of Eq. (31) is given by

$$\alpha'' + \alpha/(U^2) = 2C_{\rm m}/(\pi\mu r_\alpha^2) + \bar{F}\sin(k\tau), \tag{33}$$

where, the prime ($'$) denotes the derivative with respect to non dimensional time $\tau = t\bar{V}/b$. Next, the non dimensionalized wind velocity is given by

$$U(\tau) = \frac{1}{b\omega_\alpha}\sqrt{V_{\rm rot}^2 + (V_g + V(t))^2}, \qquad t = \tau\, b/\bar{V}, \tag{34}$$

and $V(t)$ describes random fluctuations of gusts around the mean V_g. It is often modeled as a stationary, zero mean, Gaussian process. In this example, we will assume that $V(t)$ has Davenport spectrum, see Appendix II. In Eq. (33), C_m is the pitching moment coefficient, $\bar{F}$ is the non dimensional moment amplitude, $k = \omega b/\bar{V}$ is the reduced frequency of forcing, μ is mass ratio given by $\mu = m/(\pi\rho b^2)$ and r_α is the radius of gyration $r_\alpha = I_\alpha/(mb^2)$. The non dimensional parameter values considered in the numerical example are $r_\alpha = 0.5$, $\mu = 100$, $\bar{F} = 0.001$ and $k = 0.286$. An Onera dynamic stall model has been used to calculate the aerodynamic loads ($C_{\rm m}$); see [26]. Here, the aerodynamic loads depend on the instantaneous pitch and the pitch rate of the turbine blade. It is quite obvious that this is a problem in fluid-structure

interaction and is a highly nonlinear system. Some details of the aerodynamic calculations are provided in Appendix III.

The oscillations in pitching of the turbine blade contribute to fatigue damage in the blade section. We assume that the instantaneous stress developed in a turbine blade is proportional to the instantaneous pitch $\alpha(t)$. Since the crossing intensity of $\alpha(t)$ is not known, the nominal damage rate d will be estimated from a long simulation of the pitch response $\alpha(t)$, obtained by numerically integrating the governing nonlinear differential equations. It must be remarked here that because of the nonlinearity in the system, for certain initial conditions, the system exhibits self sustained oscillations even in the absence of any forcing.

4.2.1 Dependence of the damage rate on the mean gust speed V_g

We first investigate the dependence of the damage rate d on the average gust speed V_g. We begin with the simplified situation where the effect of temporal fluctuations of the gusts is neglected, *i.e.*, $V(t) = 0$ in Eq. (34). Consequently, the damage rate for the turbine blade depends only on the non dimensional velocity

$$U = \bar{V}/b\omega_\alpha. \tag{35}$$

We compute the damage rate as a function of U and the results are shown in Fig. 6. From the figure, we see that the damage rate d depends on U in a very complex way. This seems to indicate that the behavior of the dynamical system for different values of U are significantly different.

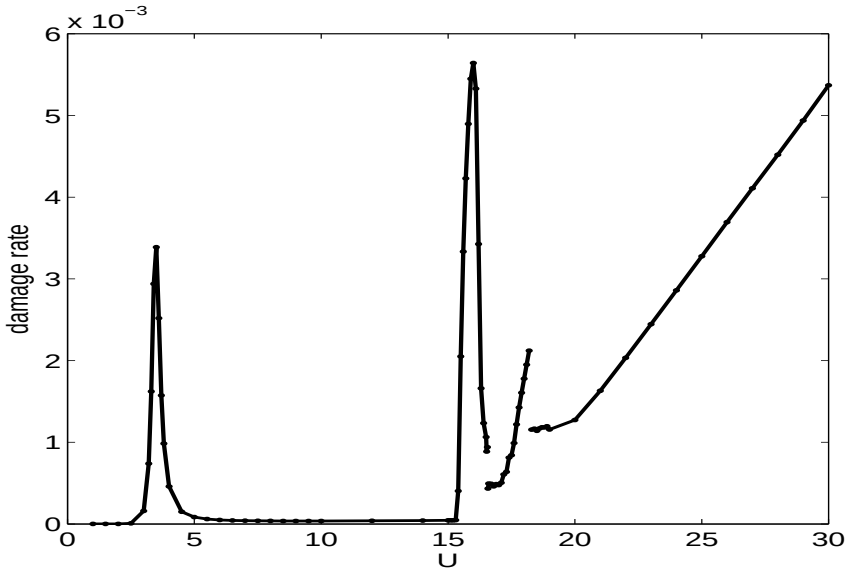

Fig. 6. Example 3: Wind turbine blade. Damage rate d as a function of non dimensional velocity U (gusts are neglected).

To explain this very surprising relationship between the damage rate and U, we carry out a bifurcation analysis for the turbine blade dynamical system. The bifurcation analysis involves studying the long term dynamical behavior of the nonlinear dynamical system with respect to a particular system parameter. In this study, we consider U to be the bifurcation parameter and study the long term response as U is varied deterministically from 0 to 30.

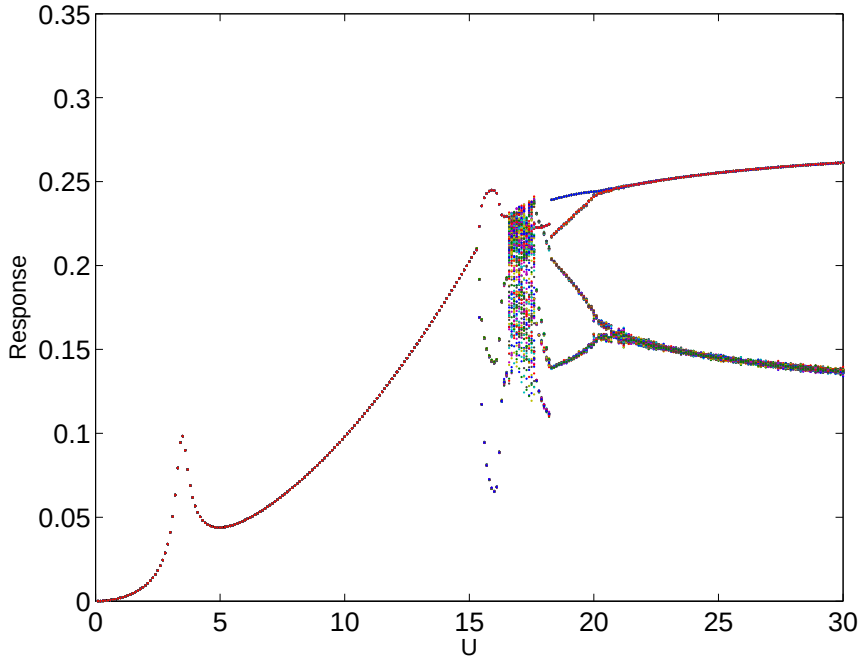

Fig. 7. Example 3: Wind turbine blade. The bifurcation diagram of the response $\alpha(t)$ with U being the bifurcation parameter.

The bifurcation diagram in Fig. 7 is constructed by plotting the maxima of the long term response in a large number of consecutive cycles. In the absence of any random gusts, the system essentially exhibits cyclic response whose amplitude and frequency depend on the system parameters and U. From Fig. 7, we see that as U increases, the amplitude of the response sinusoids also increases. For $U < 15$, the response exhibits a periodic behavior and the maxima of the consecutive cycles are coincident on the bifurcation diagram in Fig. 7. A possible reason for the peak at $U = 4$ is that at low values of U, the nonlinear effects in the system are negligible and the peak is due to resonance of the predominantly linear system. The increased fatigue damage rate is also observed in Fig. 6 where in the same range of U we observe a similar peak.

However, as U is increased beyond ≈ 15, we observe that there are two branches in the bifurcation diagram indicating that the response contains two amplitudes in a cyclic period. This period doubling indicates a qualitative change in the dynamical behavior and the value of U which marks the onset of this behavior is termed as the bifurcation point. The two branches in the bifurcation diagram are obtained from the two amplitudes within the

new period-2 cycle. Here, the maximum values of every alternate cycles are coincident. In the chaotic regime, the system response is no longer periodic; consequently, none of the maxima of the cycles are coincident in the bifurcation diagram. The chaotic regime can be seen in the range $U \approx [16, 18]$ in Fig. 7.

The complex relationship between damage rate d and U and the sudden qualitative changes in the damage rates, as shown in Fig. 6, mirrors the bifurcation points in Fig. 7. A more thorough study needs to be carried out to gain further insights into the reasons of the complex relationship between damage rate d and U. It is to be noted here that the relationship between d and U contains multiple spikes and even exhibits sharp discontinuities. It is therefore quite obvious that a large number of terms would be required if Hermite polynomials are used for the expansion leading to slow convergence. Hence, this method is not an appropriate technique to model the complex dependence between U and the damage rate.

For the turbine rotating with the rated speed of 25.4 RPM and average head wind V_g below 25 m/s, the non dimensional speed U is between 16.1 and 17.9. As is evident from Fig. 7, this interval coincides with the region of chaotic behavior of the system and relatively low damage rates, see Fig. 6. The second typical situation is when rotor is at rest i.e. $V_{\text{rot}} = 0$ m/s, i.e. $\bar{V} = V_g$. For rotor at rest and the mean gusts $V_g \leq 45$ m/s, the non dimensional speed U is below 14.5 and the only region with high damage rates is when $9 < V_g < 11$ m/s. It seems that the blade parameters are well chosen in respect to minimizing the risk against fatigue damages.

4.3 Influence of random gust fluctuations on fatigue damage rate

We next study the influence of gusts fluctuations on the nominal damage rate in the turbine blades. We assume that the gusts fluctuations are zero mean Gaussian processes with Davenport spectrum. We once again consider the two cases (a) turbine is operating with the speed of 25.4 RPM, such that, $V_{\text{rot}} = 50$ m/s and (b) when rotor is at rest *i.e.*, $V_{\text{rot}} = 0$ m/s. The corresponding damage rates d as a function of U, for the two cases, are respectively shown in Figs. 8-9.

From Figs. 8-9, we observe that when the random temporal fluctuations in the gusts are included in the fatigue damage computations, the dependence of the damage rate d on the mean gusts speed V_g is smoothened to the extent that one can respectively use the Hermite polynomials of 7th order (rotor at rest; Fig. 8) and 5th order (rotor working at 25.4 RPM; Fig. 9) to describe the dependence. In order to fit the Hermite polynomial chaos expansions, we

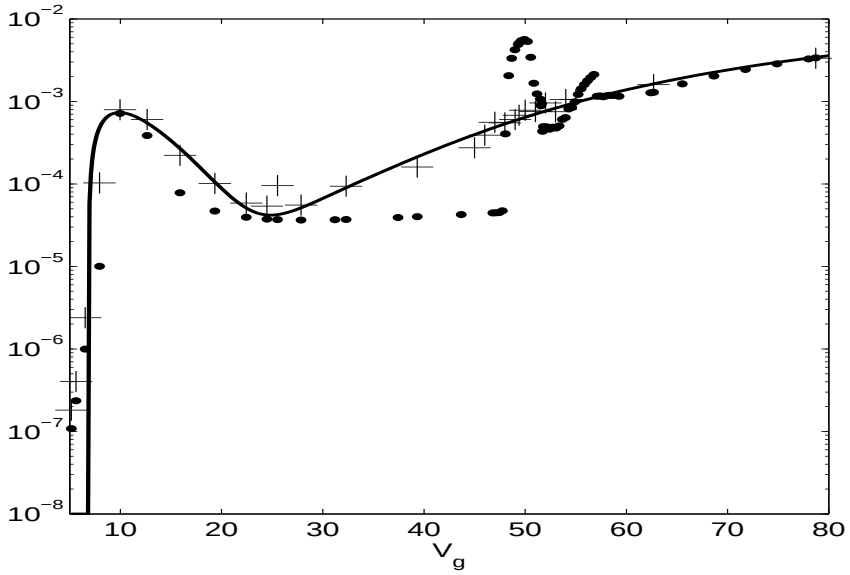

Fig. 8. Example 3: Wind turbine blade. y-axis: The damage rate d as a function of the mean wind speed V_g (with gusts $V(t)$ having Davenport spectrum); Rotor at rest, *i.e.*, $V_{\text{rot}} = 0$ m/s; Dots: damage rates obtained when gusts fluctuations are neglected (taken from Fig. 6); Crosses: estimated damage rates with variable gusts; Solid line: Hermite polynomial approximations of 7th order; note: y-axis is in the log-scale.

assumed that V_g is an uncertain parameter, modeled as

$$\ln V_g = m + \sigma\, Z, \qquad Z \in \mathcal{N}(0,1), \tag{36}$$

and $m = 25$ and $\sigma = 0.4$. Note that here we are not modeling the temporal variations in gusts as a random process; instead we adopt the simpler random variable model and assume that all the uncertainties associated with the gusts can be adequately represented through the single random variable Z. Since $Z = (\ln(V_g) - m)/\sigma$, the fitted models for $d(V_g)$ are respectively 7th and 5th order Hermite polynomials in $\ln(V_g)$. (Note that using Hermite polynomials in the Weiner chaos expansions is not optimal). This way of choosing the functional relations gives higher accuracy model in the region of interest, *e.g.*, the maximal operational speed of the rotor 25 m/s. Obviously other methods of fitting the relation could be used. However, due to the complex dependence structure, the Gauss error propagation formula gives very poor description of $d(Z)$ (or $d(V_g)$) and are not applicable.

Finally note that the influence of $V(\tau)$ on $U(\tau)$, see Eq. (34), is much higher for the rotor at rest. Neglecting the gust would lead to an underestimation of the damage rates, at least for some values of U. Otherwise, the damage rates are somewhat unaffected by gust. Overall, the influence of the gust has been in smoothening the damage rates and as a result the sharp peaks are absent from the damage rate behavior with gust. It is indeed interesting that the damage

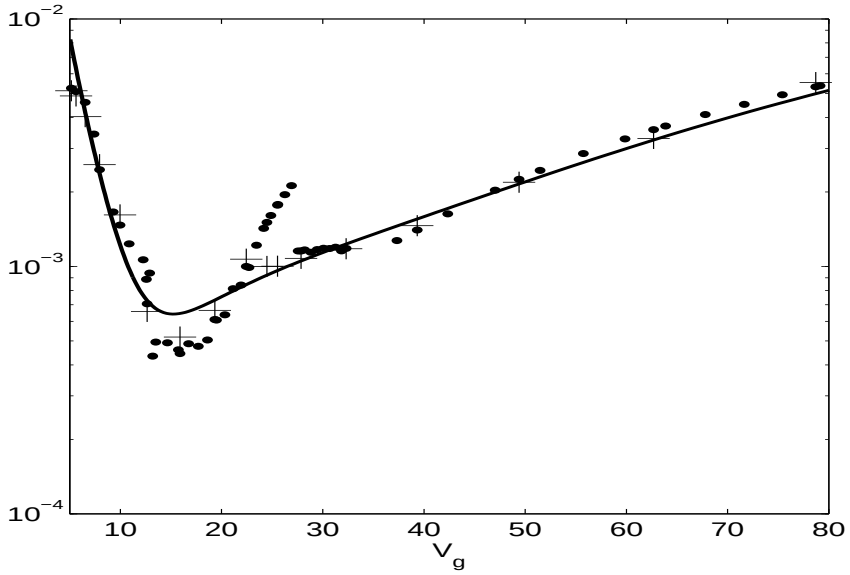

Fig. 9. Example 3: Wind turbine blade. y-axis: The damage rate d as a function of the mean wind speed V_g (with gusts $V(t)$ having Davenport spectrum); Rotor working with 25.4 RPM, *i.e.*, $V_{\rm rot} = 50$ m/s; Dots: damage rates obtained when gusts fluctuations are neglected (taken from Figure 6); Crosses: estimated damage rates with variable gusts; Solid line: Hermite polynomial approximations of 5th order; note: y-axis is in the log-scale.

rate should rise sharply at some U values in the absence of gust and does not do so with gust. For example, if we consider the case of rotating blades when $V_g = 27$ m/s, we observe a sharp peak around the mean wind speed when gust is absent; see Fig. 9. To understand this curious phenomenon, we compare the time histories of the response at this V_g; see Fig. 10. The corresponding nondimensional U is 18.21. From Fig. 10, we see that the response without gust manifests a period-4 behavior and is of somewhat higher amplitude than that with gust. It is clear that the response amplitude as well as the mean response is diminished in the presence of gust. The frequency of the peaks is largely unaffected. However, for the gust response which is essentially aperiodic, the use of the term frequency has been somewhat in a qualitative sense. The reason behind this should be clear from the gust time history given in Fig. 11. As can be seen here, the variation of the gust wind with respect to the non-dimensional time is rather slow. The gust therefore changes the response amplitude slowly and does not affect the frequency. This is evident from the response time history corresponding to without gust shown in Fig. 10. The fundamental forcing frequency is clearly much higher in this case which is unaffected by the slow-changing gust. This value of $V_g = 27$ m/s is a typical case where the damage rate is significantly higher owing to a large difference between the maximum and minimum values of the response. This was evident in the bifurcation plot in Fig. 7 and corresponds to the last peak in the damage rate profile in Fig. 6. For other values of V_g, where we do not encounter any such sharp rise in the damage rate in the absence of gust, the influence of gust

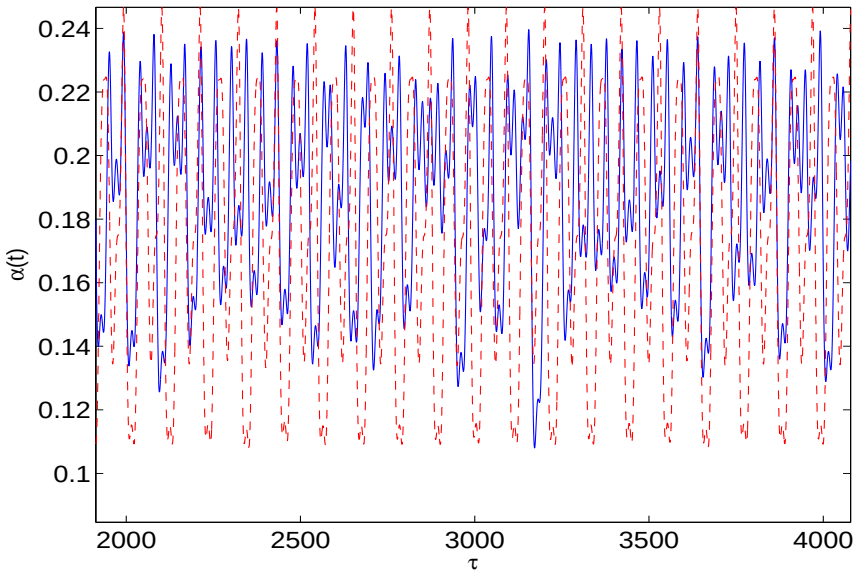

Fig. 10. Example 3: Response time histories; solid line is for response with gust; dashed line is without gust.

seems to be minimal in toning down the damage rate.

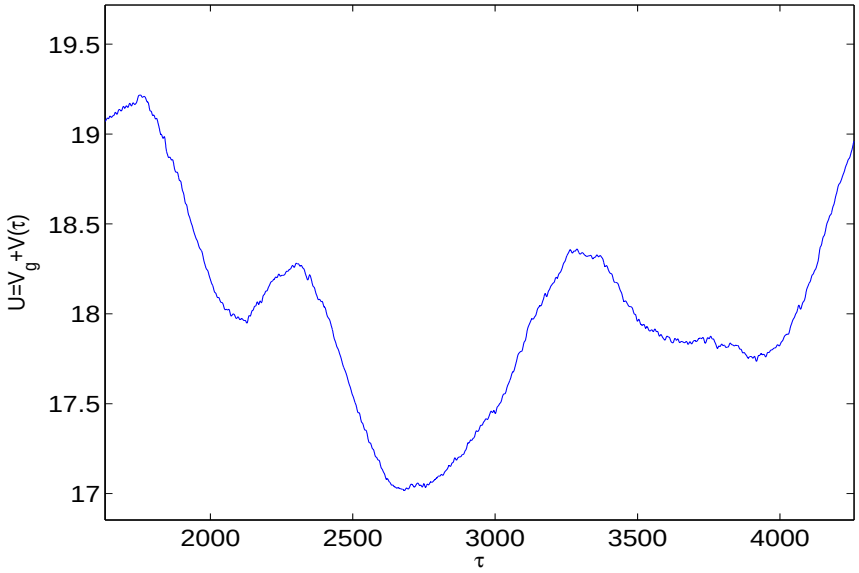

Fig. 11. Example 3: Gust time history.

5 Concluding Remarks

The study carried out in this paper investigates the use of Wiener chaos expansions for estimating the fatigue damage in vibrating structures with uncertain parameters. The loadings have been assumed to be Gaussian and stationary. The narrowband approximation discussed in the literature have been used to

estimate the fatigue damage corresponding to the mean parameters of the system. Subsequently, the effect of the parameter uncertainties on the fatigue damage has been estimated using Wiener chaos expansions. The salient features emerging from this study are summarized as follows:

- For linear structures subjected to Gaussian excitations, the performance of the proposed method is as good as the commonly used Gauss error propagation formulae.
- For non-Gaussian structural responses, the proposed method gives better accuracies in the fatigue damage rate estimates than the Gauss error propagation formula, especially when the deviations from the mean values are large.
- Though the computations involved in the proposed method are more than the simpler Gauss formula, the use of the latter requires calculating derivatives which introduce larger numerical uncertainties, especially when higher order terms are required.
- In the wind turbine problem, the uncertainties in the gust are observed to increase the fatigue damage rates significantly for lower average wind speeds, highlighting the importance of modeling the random variations in the gusts. The effect of uncertainties in structural parameters need to be investigated; however, this study has not been carried out in the present work.
- The Gauss error propagation formula is inappropriate for highly nonlinear problems (eg. the wind turbine problem) because of the complicated damage relationship with the uncertain parameter. additionally, the use of this approach demands restrictive conditions on the differentiability of the functional relationship. On the other hand, the proposed method based on Wiener chaos expansions do not place demands on the differentiability of the relationship and is hence applicable to a wider class of problems.
- The formulation and the examples presented in this work is based on only a single variable model for representing the parameter uncertainties. A single parameter uncertainty has been considered for simplicity and ease of exposition. The method can be applied with larger number of parameter uncertainties; this would however, increase the computational costs.

Acknowledgement

The research presented in this paper has been partially supported by the Gothenburg Stochastic Center and the Swedish foundation for Strategic Research through GMMC, Gothenburg Mathematical Modelling Center.

References

[1] Miner MA. Cumulative damage in fatigue. J. Applied Mechanics 1945;12:A159-A164.

[2] Palmgren A. Die Lebensdauer von Kugellagern, VDI Zeitschrift 1924;68:339-341.

[3] Paris PC, Erdogan F. A critical analysis of crack propagation laws. Journal of Basic Engineering, Transactions of the ASME 1963; D85:528-534.

[4] Bendat JS. Probability functions for random responses: Prediction of peaks, fatigue damage and catastrophic failures. Tech. rep., NASA, 1964.

[5] Rychlik I. On the "narrow-band" approximation for expected fatigue damage. Probabilist. Eng. Mech. 1993;8:1-4.

[6] Wiener N. The homogeneous chaos. Amer. J. Math. 1938; 60:897-936.

[7] Wiener N. Nonlinear problems in random theory. MIT Press, 1958.

[8] Cameron RH, Martin WT. The orthogonal development of non-linear functionals in series of Fourier-Hermite functionals. Ann. Math. 1947; 48:385-392.

[9] Ghanem R, Spanos PD. Stochastic finite element: A spectral Approach. Springer-Verlag, Berlin, 1991.

[10] Xiu D, Karniadakis G. The Wiener -Askey polynomial chaos for stochastic differential equations. SIAM Journal of Scientific Computation 2002;24(2):619-644.

[11] Winterstein SR. Non-normal responses and fatigue damage, J. Eng. Mech., ASCE 1985;111:1291-1295.

[12] Matsuishi M, Endo T. Fatigue of metals subjected to varying stresses. Paper presented to Japan Soc. Mech. Engrs, Fukuoka, Japan, 1968.

[13] Rychlik I. A new definition of the rainflow cycle counting method. Int. J. Fatigue 1987;9:119-121.

[14] Johannesson P, Svensson T, de Maré J. Fatigue life prediction based on variable amplitude tests - methodology. International Journal of Fatigue 2005l;27:954-965.

[15] Bengtsson AK, Rychlik I. Uncertainty in fatigue life prediction of structures subject to Gaussian loads. Probabilistic Engineering Mechanics 2009;24:224-235.

[16] Madsen HO, Krenk S, Lind NC. Methods of structural safety. Engelwood cliffs, New Jersey, 1986.

[17] Manohar CS, Gupta S. Modeling and evaluation of structural reliability: current status and future directions. Recent Advances in Structural Engineering, (Eds. Jagadish KS, Iyengar RN), University Press, 2005;90-187.

[18] Rice SO. The mathematical analysis of random noise i and ii. Bell Syst. Tech. J. 1944;23:282-332, 1945;24:46-156.

[19] Bogsjö K. Development of analysis tools and stochastic models of road profiles regarding their influence on heavy vehicle fatigue. Suppl. Vehicle System Dynamics 2006; 44:780-790.

[20] LaBarre RP, Forbes RT, Andrews S. The measurement and analysis of road surface roughness. Technical Report 5. Motor Industry Research Association (MIRA), 1970.

[21] Lee BHK, Price SJ, Wong YS. Nonlinear aeroelastic analysis of airfoils: bifurcation and chaos. Progress in Aerospace Sciences 1999;35:205-334.

[22] Alighanbari H, Price SJ. The post-Hopf bifurcation response of an airfoil in incompressible, two-dimensional flow. Nonlinear Dynamics 1996;10:381-400.

[23] Tang DM, Dowell EH. Nonlinear aeroelasticity in rotorcraft. Mathematical and Computer modelling 1993;18:157-184.

[24] Fragiskatos G. Nonlinear response and instabilities of a two-degree-of-freedom airfoil oscillating in dynamic stall. M.Eng. Masters Thesis, McGill University, Montreal, Canada, 1999.

[25] Fung YC. An introduction to the theory of aeroelasticity, John Wiley & Sons, Inc, 1969.

[26] Tran CT, Petot T. Semi-empirical model for the dynamic stall of airfoils in view of the application to the calculation of responses of a helicopter blade in forward flight. Vertica 1981;5:35-53.

[27] Harris RI. The Nature of the Wind, the modern Design of Wind Sensitive Structures Const. Ind. Res. & Inf. Ass., London 1971:29-55.

[28] Davenport AG. The spectrum of horizontal gustiness near the ground of high winds. Quarterly Journal Royal Meteorological Society 1961;87:194-211.

[29] Felkema GJ, Wichers JEW. The effect of wind spectra on the low-frequency motions of a moored tanker in survival condition. OTC 6605, paper presented at the 23rd Annual OTC 1991;411-430

[30] Phillips OM. The equilibrium range in the spectrum of wind generated waves. Journal of Fluid Mechanics 1958;4:426-434.

[31] Pierson WJ, Moskowitz L. A proposed spectral form for fully developed wind seas based on the similarity theory of S.A. Kitaigorodskii. Journal of Geophysical Research 1964;5181-5190.

[32] ISSC, Report of international ship structures congress committee 1. Proceedings of the International Ship Structures Congress, Delft, The Netherlands,1964.

[33] Dunn P, Dugundji J. Nonlinear stall flutter and divergence analysis of cantilevered graphite/epoxy wings. AIAA Journal 1992;30:153-162.

A Appendix I: Definition of rainflow cycle

In the rainflow cycle counting algorithm, each local maximum of the load process is paired with one particular local minimum, determined as follows (see Fig. A):

- From the local maximum, one determines the lowest values in forward and backward directions between the time point of the local maximum and the nearest points at which the load exceeds the value of the local maximum.
- The larger of these two values is the rainflow minimum paired with that specific local maximum, *i.e.*, the rainflow minimum is the least drop before reaching the value of the local maximum again on either side.
- The cycle range, h, is the difference between the local maximum and the paired rainflow minimum.

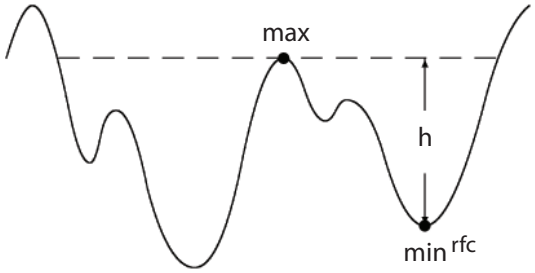

Fig. A.1. A rainflow pair

Note that for some local maxima, the corresponding rainflow minimum could lie outside the measured load sequence. In such situations, the incomplete rainflow cycle constitutes the so called residual and has to be handled separately. In this approach, we assume that, in the residual, the maxima form cycles with the preceding minima.

B Appendix II: Load spectrums used in examples 2 and 3

The external wind and wave loads often have simple spectrums dependent only on few parameters, see e.g. (B.2-B.6) given in following subsection. The three spectrums actually depend only on one parameter θ, say, and can be written in the following standardized form

$$S(\omega) = c(\theta)\tilde{S}(\omega/\theta). \tag{B.1}$$

B.1 Harris and Davenport spectrums

The Harris [27] spectrum has the following form

$$S(\omega) = \frac{7200\,C}{2\pi}\frac{\theta}{(2+(286\omega/\theta)^2)^{5/6}}, \tag{B.2}$$

where, C is the turbulence or surface drag coefficient (may be chosen equal to 0.002 for "rough" seas and 0.0015 for "moderate" seas (severity of sea is measured by means of the significant wave height H_s, approximately four standard deviations of the sea level elevation at a fixed point). Further θ is the hourly mean wind speed ($[m/s]$) at a reference level 10 m above water surface. For the wind speed on land, Davenport [28] spectrum is often used and is of the form

$$S(\omega) = \frac{916700\,C}{2\pi}\frac{\theta}{(1+(191\omega/\theta)^2)^{4/3}}. \tag{B.3}$$

For other wind spectra, see [29].

B.2 Pierson-Moskowitz spectrum

Based on the upper bound expression for the energy of wind-generated deep water gravity waves, derived by [30], and from the empirical measurements in the North Atlantic, the following spectrum for fully developed deep water sea waves has been suggested in [31] ,

$$S(\omega) = \frac{\alpha g^2}{\omega^5}\exp\left(-\beta\left(\frac{\omega_0}{\omega}\right)^4\right). \tag{B.4}$$

Here, the constants $\alpha = 0.0081$, $\beta = 0.74$ and $\omega_0 = g/V$, where V is the wind speed 19.5 m above still water sea level and g is the gravity constant. The first Pierson-Moskowitz spectrum imposes a deterministic relation between significant wave height (range) and mean wave period.

A generalized form of the P-M spectrum, allowing for independent H_s and T_z (the average zero crossing wave period), was given by [32],

$$S^{PM}(\omega) = \frac{H_s^2\theta}{4\pi}(\omega/\theta)^{-5}\exp\left(-\frac{1}{\pi}(\omega/\theta)^{-4}\right), \tag{B.5}$$

where, $\theta = 2\pi/T_z$ is the average angular frequency. For the North Atlantic, one sometimes uses an approximation $T_z = 3.5\sqrt{H_s}$. These leads to the simplified

form of the spectrum

$$S(\omega) = 13.224\,\omega^{-5} \exp\left(-\frac{1}{\pi}(\omega/\theta)^{-4}\right). \tag{B.6}$$

This is the spectrum that has been used in Section 4.1.

C Appendix III: Onera dynamic stall model

An Onera dynamic stall model [26] has been used to calculate the aerodynamic loads for the wind turbine blades. This is a semi-empirical model in which the dynamic stall loads are given in terms of a system of nonlinear differential equations. The coefficients of these equations are fitted from experimental observations; hence the name semi-empirical. We use the coefficients from [33] for a moderate to high Reynolds number case. The physical process of dynamic stall is a complex unsteady phenomenon. It involves airfoil leading and trailing edge vortex developments and their subsequent interactions and shedding into the wake. Vortex growth on the airfoil upper surface increases suction pressure and helps increase the aerodynamic loads beyond their steady counterparts. Vortex separation from the body rapidly decreases the loads. One can use the Onera model to recreate this highly interactive and nonlinear phenomenon without having to solve the complicated Navier-Stokes equations. The Onera dynamic stall equations are:

$$C_z = s_z\alpha' + k_{\mathrm{v}z}\theta'' + C_{\mathrm{z}_1} + C_{\mathrm{z}_2} \tag{C.1}$$

$$C'_{z_1} + \lambda_z C_{z_1} = \lambda_z\left(a_{\mathrm{o}z}\alpha + \sigma_z\theta'\right) + \alpha_z\left(a_{\mathrm{o}z}\alpha' + \sigma_z\theta''\right) \tag{C.2}$$

$$C''_{z_2} + 2d\omega C'_{z_2} + w^2\left(1+d^2\right)C_{z_2} = -w^2\left(1+d^2\right)\left[\Delta C_z(\alpha) + e\Delta C'_z(\alpha)\right], \tag{C.3}$$

where, the coefficients $s_z,\ k_{\mathrm{v}z},\ \lambda_z,\ \alpha_z,\ a_{\mathrm{o}z},\ \sigma_z,\ d,\ w$ and e are empirically determined by parameter identification techniques using experimental data [33]. If there is only pitching oscillation mode, α and θ are the same.

The coefficients C_z are the aerodynamic coefficient $C_{\mathrm{l}},\ C_{\mathrm{d}}$ or C_{m} for $z = \{\mathrm{l}, \mathrm{d}, \mathrm{m}\}$. In this case, only the moment coefficient C_{m} is of interest. The aerodynamic moment consists of two contributions: (i) the inviscid circulatory part C_{m_1} given by (C.2) and (ii) the viscous stall part C_{m_2} given by Eq. (C.3), which becomes important above the static stall angle. The stall behavior is modeled in Eq. (C.3) by the ΔC_{m} term. The ΔC_{m} part is a nonlinear function which is identically zero below the static stall angle of 12^{o} at which it exhibits a discontinuous step to a finite value.